

Optical study of the spin-density-wave properties of single-crystalline $\text{Na}_{1-\delta}\text{FeAs}$

W. Z. Hu, G. Li, P. Zheng, G. F. Chen, J. L. Luo, and N. L. Wang

Beijing National Laboratory for Condensed Matter Physics, Institute of Physics, Chinese Academy of Sciences, Beijing 100190, China

(Received 2 July 2009; revised manuscript received 30 August 2009; published 28 September 2009)

We report an optical investigation on the ab plane charge dynamics for $\text{Na}_{1-\delta}\text{FeAs}$ single crystal. Formation of a partial energy gap is clearly observed in the magnetic ordered phase. Comparing with the optical response of other FeAs-based parent compounds with high magnetic transition temperatures, both the gap value 2Δ and the energy scale for the gap-induced spectral weight redistribution are smaller in $\text{Na}_{1-\delta}\text{FeAs}$. The experimental results favor an itinerant origin of the antiferromagnetic transition.

DOI: [10.1103/PhysRevB.80.100507](https://doi.org/10.1103/PhysRevB.80.100507)

PACS number(s): 78.20.-e, 75.30.Fv

The interplay between different instabilities, such as structural distortions, magnetic orderings, and superconductivity, is of central interest in condensed matter physics. The discovery of superconductivity in Fe-based layered materials¹ offers a new opportunity to study the intriguing interplay between those instabilities. The undoped FeAs-based compounds commonly display the structural and magnetic phase transitions,²⁻⁴ and the magnetic order has a collinear spin structure with a (π, π) wave vector in the folded Brillouin zone (two Fe ions per unit cell). Upon electron or hole doping or application of pressure, both the magnetic order and the structural transition are suppressed, and superconductivity emerges.^{3,5,6} It is widely believed that the structural distortion is driven by the magnetic transition,^{7,8} however, there have been much debate over the origin of the magnetic order. Many theoretical works emphasize on the itinerant nature of the magnetism. That is, the magnetic transition is of the spin-density wave (SDW) type, being driven by the nesting instability of the disconnected electron and hole Fermi surfaces (FS) separated by a (π, π) wave vector.⁹⁻¹³ Alternatively, a Heisenberg model with exchange interactions between localized spin moments is suggested to explain the collinear spin structure.^{7,8,14-16} Although for a practical system both the itinerancy and the local-moment exchange interactions might be present,¹⁷ one of them may play a dominant role. A clear difference between the two mechanisms is that a single particle gap (i.e., SDW gap) would open at the FS in the broken symmetry state for the former mechanism, but not necessary for the later which basically applies to systems with localized electrons.

One of the advantages for spectroscopic techniques is to probe the energy gap in the ordered state. Previous optical investigations provide clear evidence for the formation of the partial gap in the magnetic phase in polycrystalline ReFeAsO (Re=La, Ce, Nd, etc.)^{9,18-20} and single-crystalline AFe_2As_2 (A=Ba, Sr, Eu)^{21,22} supporting the itinerant picture that the energy gain for the antiferromagnetic ground state is achieved by the opening of an SDW gap on the FS. Quantum oscillation experiment revealed three Fermi surfaces with area much smaller than those in the paramagnetic phase predicted by the local-density approximation calculation,²³ thus agree with optical observation of a large reduction in effective carrier density in the SDW state. However, angle-resolved photoemission spectroscopy (ARPES) experiments did not yield consistent results.²⁴⁻²⁷ Moreover, the iron chalcogen-based parent compound, Fe_{1+x}Te , shows no signa-

ture of the gap after the structural/magnetic transitions.²⁸ As neutron experiments revealed that the low- T magnetic phase has a bicollinear spin structure with a $(\pi, 0)$ wave vector,^{29,30} which is different from the (π, π) wave vector that connects the electron and hole pockets, the absence of gap opening below T_{SDW} is not surprising. Further spectroscopic studies are required to find out whether the gap formation is a common feature for different types of FeAs-based parent compounds.

Recently, high-quality single crystals are synthesized for almost stoichiometric $\text{Na}_{1-\delta}\text{FeAs}$, a 111-type FeAs-based parent compound. Separated structural/magnetic transitions at 52 and 41 K, together with a superconducting transition at 23 K are observed by transport measurements.^{31,32} Here we report the ab plane optical properties for $\text{Na}_{1-\delta}\text{FeAs}$ single crystal. Similar to other FeAs-based parent compounds, clear evidence for the SDW gap is found, and a residual Drude term (free-carrier response) is seen in the SDW ordered phase. Therefore, the metallic response and the SDW gap are common features for all known FeAs-based parent compounds. The gap value 2Δ has a smaller energy scale than that of the 122-type compounds, in which higher SDW transition temperatures are found. The ratio of $2\Delta/k_B T_{\text{SDW}} \approx 4.2$ is close to the expectation of mean field theory for an itinerant SDW order.

Single crystalline $\text{Na}_{1-\delta}\text{FeAs}$ samples were grown by the self-flux method.³¹ The obtained crystals can be easily cleaved along ab plane. The dc resistivity $\rho(T)$ is obtained by the standard four-probe method on a sample cleaved from the same crystal used in the optical measurement. The result is shown in Fig. 1. Two transitions near 40 and 50 K were assigned to separated structural and magnetic transitions,³¹ which were confirmed by recent neutron diffraction measurement.³³ Here the dc resistivity turns up after the structural distortion, and increases more rapidly with decreasing T below the magnetic transition. A superconducting transition is seen with an onset temperature of 25 K, and a zero resistivity is approached when $T \leq 10$ K. This was interpreted as due to the slight Na deficiency (less than 1%).³¹ However, specific-heat measurement shows no detectable anomaly near T_c .³¹ Neutron measurement on the identically prepared crystals also indicates no anomaly across T_c for the antiferromagnetic order parameter.³³ These results suggest that superconductivity in the sample is filamentary and not a bulk phenomenon. Therefore, the optical data are dominated by the response of the parent phase.

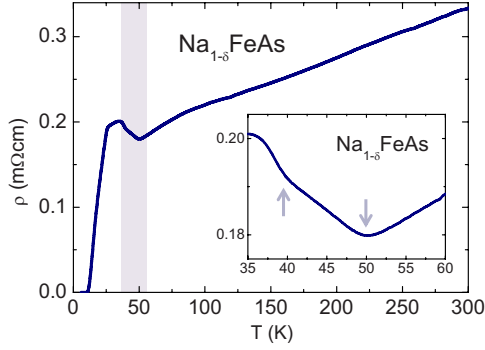


FIG. 1. (Color online) The *ab* plane dc resistivity for $\text{Na}_{1-\delta}\text{FeAs}$ single crystal. Inset: two separated transitions around 40 and 50 K.

The optical reflectance measurements were performed on a combination of Bruker IFS 66v/s and 113v spectrometers on newly cleaved surfaces (*ab* plane) in the frequency range from 40 to 25000 cm^{-1} . An *in situ* gold and aluminum overcoating technique was used to get the reflectivity $R(\omega)$. The real part of conductivity $\sigma_1(\omega)$ is obtained by the Kramers-Kronig transformation of $R(\omega)$.

Figure 2 shows the room-temperature optical reflectivity and conductivity spectra over broad frequencies up to 25000 cm^{-1} . The overall spectral lineshapes are very similar to AFe_2As_2 ($A=\text{Ba}, \text{Sr}$) single crystals. As a comparison, we have included the optical data on BaFe_2As_2 in the figure.²¹ The reflectance drops almost linearly with frequency at low- ω region, then merges into the high values of a background contributed mostly from the interband transitions from the midinfrared to visible regime. By fitting the conductivity spectrum with the Drude and Lorentz model in a way similar to what we did for 122-type crystals,²¹ we get the plasma frequency $\omega_p \approx 10200 \text{ cm}^{-1}$ and scattering rate $1/\tau \approx 660 \text{ cm}^{-1}$ for $\text{Na}_{1-\delta}\text{FeAs}$. Both are comparable to the parameters found for the 122-type materials.^{21,22} This indicates that we are measuring the charge dynamics of Fe_2As_2 layers.

Figure 3 shows the optical reflectivity $R(\omega)$ for

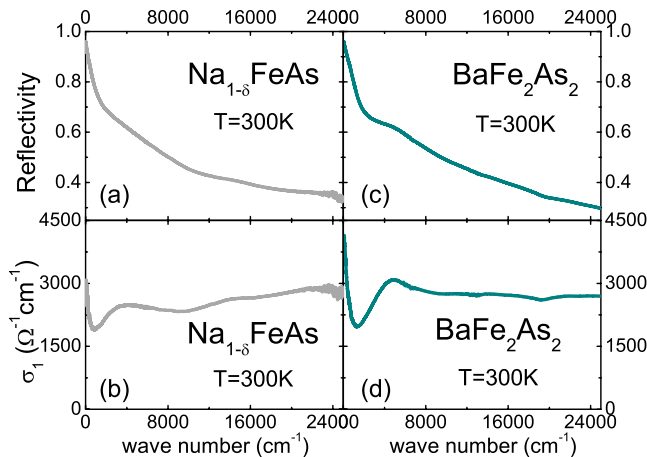


FIG. 2. (Color online) The room-temperature optical reflectivity (a) and conductivity (b) for $\text{Na}_{1-\delta}\text{FeAs}$ single crystal over broad frequencies up to 25000 cm^{-1} . Data on BaFe_2As_2 ²¹ are shown in (c) and (d) for comparison.

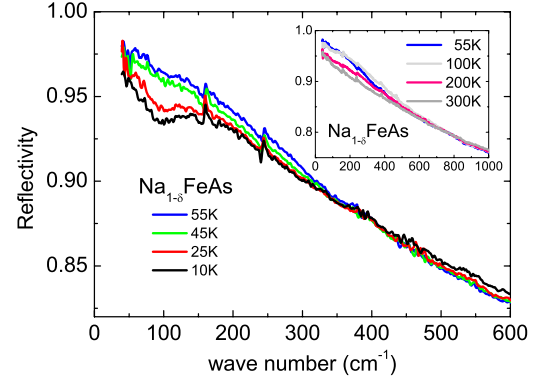


FIG. 3. (Color online) Optical reflectivity $R(\omega)$ below 600 cm^{-1} for $T \leq 55 \text{ K}$. The SDW gap is evidenced by a spectral suppression in the far infrared for $T=10$ and 25 K. Inset: $R(\omega)$ below 1000 cm^{-1} for 55, 100, 200, and 300 K.

$\text{Na}_{1-\delta}\text{FeAs}$ below 600 cm^{-1} . Two phonons around 160 and 244 cm^{-1} can be found. $R(\omega)$ at low T decreases gradually below 400 cm^{-1} , consists with the increasing of $\rho(T)$ below 50 K. In the SDW state, a suppression in $R(\omega)$ below 150 cm^{-1} is observed, indicating the opening of an SDW gap on the Fermi surface. Similar cases were found for the undoped 122-type^{21,22,34} and 1111-type^{19,20} compounds. The inset plots the low-frequency $R(\omega)$ for $T=55, 100, 200,$ and 300 K. Here $R(\omega)$ shows a metallic response in the far-infrared region, that the reflectivity continues to grow with lowering T in the normal state, in agreement with the metallic response as seen in the dc resistivity.

The low- ω temperature-dependent real part of conductivity $\sigma_1(\omega)$ is shown in Fig. 4. Besides two sharp phonon modes around 160 and 244 cm^{-1} , $\sigma_1(\omega)$ for both $T=45$ and 55 K show a Drude response without any clear evidence for the gap-induced absorption peak. For $T=10$ and 25 K, a peak with a clear edgelike feature is formed around 120 cm^{-1} . Meanwhile, a remaining Drude component is seen below 80 cm^{-1} , indicating that the Fermi surface is only partially gapped and $\text{Na}_{1-\delta}\text{FeAs}$ is still metallic in the SDW state.

The optical conductivity $\sigma_1(\omega)$ shows different gap characters for the superconducting and the density wave states

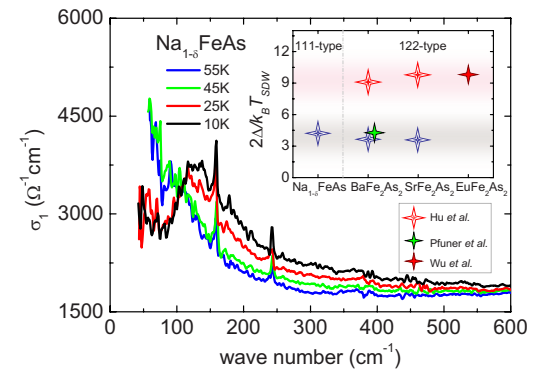


FIG. 4. (Color online) The real part of optical conductivity $\sigma_1(\omega)$ for $\text{Na}_{1-\delta}\text{FeAs}$ below 600 cm^{-1} . An SDW gap emerges for $T < T_{\text{SDW}}$. Inset: $2\Delta/k_B T_{\text{SDW}}$ for $\text{Na}_{1-\delta}\text{FeAs}$ (this study), BaFe_2As_2 [Hu *et al.*, (Ref. 21)] SrFe_2As_2 [Pfner *et al.* (Ref. 34)], SrFe_2As_2 [Hu *et al.* (Ref. 21)] and EuFe_2As_2 [Wu *et al.* (Ref. 22)].

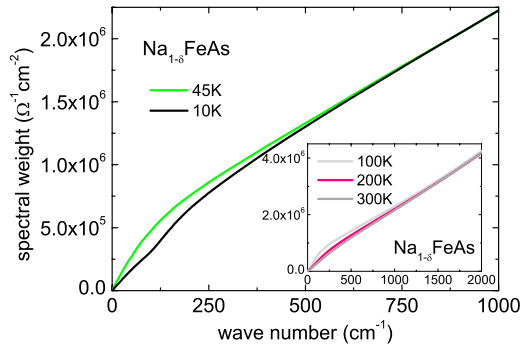


FIG. 5. (Color online) The spectral weight $\int_0^\omega \sigma_1(\omega) d\omega$ for $\text{Na}_{1-\delta}\text{FeAs}$ below 1000 cm^{-1} for $T=10$ and 45 K . Inset: the spectral weight for $T=100, 200,$ and 300 K up to 2000 cm^{-1} .

due to their respective coherence factors.^{35,36} For the SDW ground state with an isotropic gap, a nonsymmetric peak with clear edgeline feature emerges at 2Δ in the optical conductivity,^{37,38} so that $\sigma_1^{\text{SDW}}(\omega)$ exceeds the normal state conductivity $\sigma_1^{\text{N}}(\omega)$ at the gap onset,³⁵ above which the loss in free-carrier (Drude) spectral weight is gradually compensated by the gap-induced absorption peak. For a multiband system, gap anisotropy will weaken the edgeline feature at 2Δ . Here we use the peak position (the conductivity maximum) to estimate the SDW gap. For $\text{Na}_{1-\delta}\text{FeAs}$, the conductivity peak at 10 K is around 120 cm^{-1} , i.e., $2\Delta \approx 15 \text{ meV}$ and $2\Delta/k_B T_{\text{SDW}} \approx 4.2$. Such a gap is obviously smaller than that in AFe_2As_2 and ReFeAsO .^{19–22,34} In the inset of Fig. 4 we show $2\Delta/k_B T_{\text{SDW}}$ obtained by optical data on 111 ($\text{Na}_{1-\delta}\text{FeAs}$) and 122 (AFe_2As_2 , $A=\text{Sr, Ba, Eu}$)^{21,22,34} type parent compounds. Here the gap 2Δ for different FeAs systems are all defined by the peak positions in $\sigma_1(\omega)$ for consistency.

Besides the gap value, the spectral range affected by the SDW gap is also smaller for $\text{Na}_{1-\delta}\text{FeAs}$ in comparison with other FeAs-based parent compounds with higher T_{SDW} s. Figure 5 plots the spectral weight at 10 and 45 K for $\text{Na}_{1-\delta}\text{FeAs}$. The inset shows the spectral weight at $T=100, 200$ and 300 K . Note $\text{Na}_{1-\delta}\text{FeAs}$ is metallic in the normal state (Fig. 1), so the spectral weight piles up at low frequencies with decreasing T , which is due to an increasing dc conductivity [$\sigma_1(0)$] thus a growing Drude peak in $\sigma_1(\omega)$. Above 1700 cm^{-1} , the spectral weight for all temperatures merge together. In the SDW state, the spectral weight is smaller for 10 K than that of 45 K , indicating a loss in the Drude weight at 10 K , that part of the free carriers are removed from E_F due to the SDW gap. The spectral weight loss in low frequencies is compensated when ω approaches 750 cm^{-1} . Such an energy scale is

smaller than that of AFe_2As_2 (e.g., 2000 cm^{-1} for BaFe_2As_2 where $T_{\text{SDW}} \approx 140 \text{ K}$).²¹

Our study indicates that the metallic response and the opening of an energy gap in the magnetic ordered state are common behaviors for all FeAs-based undoped compounds, and the gap size correlates with T_{SDW} . Associated with the gapping of the Fermi surface, a large part of the Drude component is removed (indicating a reduction in the FS area), therefore results in a spectral weight transfer from the Drude term into the gap-induced absorption peak in $\sigma_1(\omega)$. All favor an itinerant origin of the antiferromagnetic order for FeAs-based parent compound. We noticed that some ARPES studies^{25,27} on BaFe_2As_2 did not reveal any gap in the SDW state, therefore failed to see a dramatic reduction in Fermi surface areas. As the optics probes the bulk properties, while the ARPES is mainly a surface probe, it remains to clarify if there is a surface reconstruction which would affect the results. Considering the multiband/orbital character for FeAs-based compounds, the entire band structure might be reconstructed when parts of them were modified by FS nesting instability. In this sense, our optical data do not conflict with the band reconstruction picture.

Finally, we comment on the upturn behavior of the dc resistivity below the structural/magnetic phase transitions. Note $\rho(T)$ turns up for $\text{Na}_{1-\delta}\text{FeAs}$ but drops more steeply when $T < T_{\text{SDW}}$ for AFe_2As_2 and ReFeAsO . From the semi-classic Boltzmann transport theory, the resistivity is determined by the complex function of Fermi velocity, the scattering rate, and their weighted integral over the whole FS.³⁹ In the case of electron gas, it could be simplified to the Drude form for which the resistivity is determined by carrier density and scattering rate. Whether ρ shows an upturn or a fast drop depends on the balance of those quantities which experience substantial changes across the transition, but the essential physics is the same.

To summarize, we studied the *ab* plane optical properties for $\text{Na}_{1-\delta}\text{FeAs}$. It shares similar optical response over broad frequencies with other FeAs-based parent systems. An energy gap in $\sigma_1(\omega)$ is observed below the magnetic phase transition, accompanied by a spectral weight transfer from the free-carrier Drude term to energies above this gap. Both the gap 2Δ and the energy scale associated with the spectral weight redistribution are smaller in comparison with other undoped FeAs-based compounds with higher transition temperatures. Our findings further support that the antiferromagnetic transition in the undoped FeAs-based systems has a dominantly itinerant origin.

This work is supported by the NSFC, CAS, and the 973 project of the MOST of China.

¹Y. Kamihara, T. Watanabe, M. Hirano, and H. Hosono, *J. Am. Chem. Soc.* **130**, 3296 (2008).

²Clarina de la Cruz, Q. Huang, J. W. Lynn, Jiying Li, W. Ratcliff II, J. L. Zarestky, H. A. Mook, G. F. Chen, J. L. Luo, N. L. Wang, and Pengcheng Dai, *Nature (London)* **453**, 899 (2008).

³M. Rotter, M. Tegel, and D. Johrendt, *Phys. Rev. Lett.* **101**, 107006 (2008).

⁴J. H. Chu, J. G. Analytis, C. Kucharczyk, and I. R. Fisher, *Phys. Rev. B* **79**, 014506 (2009).

⁵Jun Zhao, Q. Huang, Clarina de la Cruz, Shiliang Li, J. W. Lynn,

- Y. Chen, M. A. Green, G. F. Chen, G. Li, Z. Li, J. L. Luo, N. L. Wang, and Pengcheng Dai, *Nature Mater.* **7**, 953 (2008).
- ⁶M. S. Torikachvili, S. L. Bud'ko, N. Ni, and P. C. Canfield, *Phys. Rev. Lett.* **101**, 057006 (2008).
- ⁷T. Yildirim, *Phys. Rev. Lett.* **101**, 057010 (2008).
- ⁸C. Fang, H. Yao, W.-F. Tsai, J. P. Hu, and S. A. Kivelson, *Phys. Rev. B* **77**, 224509 (2008); C. Xu, M. Muller, and S. Sachdev, *ibid.* **78**, 020501(R) (2008).
- ⁹J. Dong, H. J. Zhang, G. Xu, Z. Li, G. Li, W. Z. Hu, D. Wu, G. F. Chen, X. Dai, J. L. Luo, Z. Fang, and N. L. Wang, *Europhys. Lett.* **83**, 27006 (2008).
- ¹⁰I. I. Mazin, D. J. Singh, M. D. Johannes, and M. H. Du, *Phys. Rev. Lett.* **101**, 057003 (2008).
- ¹¹Y. Ran, F. Wang, H. Zhai, A. Vishwanath, and D.-H. Lee, *Phys. Rev. B* **79**, 014505 (2009).
- ¹²V. Cvetkovic and Z. Tesanovic, *Europhys. Lett.* **85**, 37002 (2009).
- ¹³D. J. Singh, *Physica C* **469**, 418 (2009) and references therein.
- ¹⁴Q. Si and E. Abrahams, *Phys. Rev. Lett.* **101**, 076401 (2008).
- ¹⁵F. J. Ma, Z. Y. Lu, and T. Xiang, *Phys. Rev. B* **78**, 224517 (2008).
- ¹⁶J. Wu, P. Phillips, and A. H. Castro Neto, *Phys. Rev. Lett.* **101**, 126401 (2008).
- ¹⁷M. D. Johannes and I. I. Mazin, *Phys. Rev. B* **79**, 220510(R) (2009).
- ¹⁸G. F. Chen, Z. Li, D. Wu, G. Li, W. Z. Hu, J. Dong, P. Zheng, J. L. Luo, and N. L. Wang, *Phys. Rev. Lett.* **100**, 247002 (2008).
- ¹⁹W. Z. Hu, Q. M. Zhang, and N. L. Wang, *Physica C* **469**, 545 (2009).
- ²⁰A. V. Boris, N. N. Kovaleva, S. S. A. Seo, J. S. Kim, P. Popovich, Y. Matiks, R. K. Kremer, and B. Keimer, *Phys. Rev. Lett.* **102**, 027001 (2009).
- ²¹W. Z. Hu, J. Dong, G. Li, Z. Li, P. Zheng, G. F. Chen, J. L. Luo, and N. L. Wang, *Phys. Rev. Lett.* **101**, 257005 (2008).
- ²²D. Wu, N. Barišić, N. Driehko, S. Kaiser, A. Faridian, M. Dressel, S. Jiang, Z. Ren, L. J. Li, G. H. Cao, Z. A. Xu, H. S. Jeevan, and P. Gegenwart, *Phys. Rev. B* **79**, 155103 (2009).
- ²³Suchitra E. Sebastian, J. Gillett, N. Harrison, P. H. C. Lau, D. J. Singh, C. H. Mielke, and G. G. Lonzarich, *J. Phys.: Condens. Matter* **20**, 422203 (2008).
- ²⁴C. Liu, G. D. Samolyuk, Y. Lee, N. Ni, T. Kondo, A. F. Santander-Syro, S. L. Bud'ko, J. L. McChesney, E. Rotenberg, T. Valla, A. V. Fedorov, P. C. Canfield, B. N. Harmon, and A. Kaminski, *Phys. Rev. Lett.* **101**, 177005 (2008).
- ²⁵L. X. Yang, Y. Zhang, H. W. Ou, J. F. Zhao, D. W. Shen, B. Zhou, J. Wei, F. Chen, M. Xu, C. He, Y. Chen, Z. D. Wang, X. F. Wang, T. Wu, G. Wu, X. H. Chen, M. Arita, K. Shimada, M. Taniguchi, Z. Y. Lu, T. Xiang, and D. L. Feng, *Phys. Rev. Lett.* **102**, 107002 (2009).
- ²⁶D. Hsieh, Y. Xia, L. Wray, D. Qian, K. K. Gomes, A. Yazdani, G. F. Chen, J. L. Luo, N. L. Wang, and M. Z. Hasan, arXiv:0812.2289 (unpublished).
- ²⁷Guodong Liu, Haiyun Liu, Lin Zhao, Wentao Zhang, Xiaowen Jia, Jianqiao Meng, Xiaoli Dong, G. F. Chen, Guiling Wang, Yong Zhou, Yong Zhu, Xiaoyang Wang, Zuyan Xu, Chuangtian Chen, and X. J. Zhou, arXiv:0904.0677 (unpublished).
- ²⁸G. F. Chen, Z. G. Chen, J. Dong, W. Z. Hu, G. Li, X. D. Zhang, P. Zheng, J. L. Luo, and N. L. Wang, *Phys. Rev. B* **79**, 140509(R) (2009).
- ²⁹W. Bao, Y. Qiu, Q. Huang, M. A. Green, P. Zajdel, M. R. Fitzsimmons, M. Zhernenkov, S. Chang, M. Fang, B. Qian, E. K. Vehstedt, J. Yang, H. M. Pham, L. Spinu, and Z. Q. Mao, *Phys. Rev. Lett.* **102**, 247001 (2009).
- ³⁰S. Li, C. de la Cruz, Q. Huang, Y. Chen, J. W. Lynn, Jiangping Hu, Yi-Lin Huang, Fong-chi Hsu, Kuo-Wei Yeh, Maw-Kuen Wu, and Pengcheng Dai, *Phys. Rev. B* **79**, 054503 (2009).
- ³¹G. F. Chen, W. Z. Hu, J. L. Luo, and N. L. Wang, *Phys. Rev. Lett.* **102**, 227004 (2009).
- ³²D. R. Parker, M. J. Pitcher, P. J. Baker, I. Franke, T. Lancaster, S. J. Blundell, and S. J. Clarke, *Chem. Commun. (Cambridge)* (2009), 2189.
- ³³S. Li, C. de la Cruz, Q. Huang, G. F. Chen, T.-L. Xia, J. L. Luo, N. L. Wang, and P. Dai, *Phys. Rev. B* **80**, 020504(R) (2009).
- ³⁴F. Pfuner, J. G. Analytis, J.-H. Chu, I. R. Fisher, and L. Degiorgi, *Eur. Phys. J. B* **67**, 513 (2009).
- ³⁵G. Grüner, *Density Waves in Solids* (Addison-Wesley, Reading, MA, 1994).
- ³⁶M. Tinkham, *Introduction to Superconductivity*, 2nd ed. (McGraw-Hill, New York, 1996).
- ³⁷L. Degiorgi, M. Dressel, A. Schwartz, B. Alavi, and G. Grüner, *Phys. Rev. Lett.* **76**, 3838 (1996).
- ³⁸V. Vescoli, L. Degiorgi, M. Dressel, A. Schwartz, W. Henderson, B. Alavi, G. Grüner, J. Brinckmann, and A. Virosztek, *Phys. Rev. B* **60**, 8019 (1999).
- ³⁹M. Dressel and G. Grüner, *Electrodynamics of Solids* (Cambridge University Press, Cambridge, 2002).